Risk variant in miR-544a binding site in *CCDC170* is associated with osteoporosis

Xinhong Liu[1,2,3,4‡], Yang Wang[5‡], Qin Tan[1,2], Yunqi He[1,2], Xin Zhao[2,3,4*]

[1] College of Biological and Chemical Engineering, Chongqing University of Education, Chongqing 400067, P.R. China

[2] Chongqing Collaborative Innovation Center for Functional Food, Chongqing University of Education, Chongqing 400067, P.R. China

[3] Chongqing Engineering Research Center of Functional Food, Chongqing University of Education, Chongqing 400067, P.R. China

[4] Chongqing Engineering Laboratory for Research and Development of Functional Food, Chongqing University of Education, Chongqing 400067, P.R. China

[5] Department of Orthopaedics, the People's Hospital of Leshan Central District, Lechan 614000, P.R. China

*Corresponding author

E-mail addresses: zhaoxin@cque.edu.cn

Funding:

The present research was supported by the Program for Innovation Team Building at Institutions of Higher Education in Chongqing (CXTDX201601040), China.

Abstract

MicroRNAs (miRNAs) play essential roles in regulating bone formation and homeostasis. Genomic variations within miRNA target sites may therefore be important sources of genetic differences in osteoporosis risk. To investigate this possibility, we searched for miRNA recognition sites within genes using the TargetScan, miRNASNP and miRbase databases. In this study, we showed that miR-544a differentially regulated the allele variants of rs6932603 in the *CCDC170* 3 ′ untranslated (3′-UTR). We also showed that miR-544a suppressed osteogenesis and promoted osteoclastogenesis by regulating the expressions of *Runx2*, *Osterix, Alp, Col1a1*, *Osteopontin* (*OPN*) ,*Osteocalcin* (*OCN*) and *Osteoprotegerin* (*OPG*). Our results suggest that allele-specific regulation of *CCDC170* by miR-544a explains the observed disease risk, and provides a potential therapeutic target for osteoporosis therapy.

Introduction

Osteoporosis is a common disease characterized by low bone mass and defects in the microarchitecture of bone tissue, which impairs bone strength and leads to an increased risk of fragility fracture responses［1］. With increased age and changes in body hormones, the body's bone mass decreases. When bone mass decreases and bone fragility increases, fractures and osteoporosis will eventually occur［2］. Discovering genetic variation loci and clarifying their biological functions in bone mineral density (BMD) variations are important to understanding the etiology of osteoporosis and developing new approaches to screen, prevent, and treat osteoporosi［3］.

MicroRNAs (miRNAs) are single-stranded noncoding RNA molecules of approximately 21–23 nucleotides long, which participate in posttranscriptional regulation of gene expression by directly binding to the 3′ untranslated region (3′-UTR) of target mRNAs［4-7］. MiRNAs play important roles in the occurrence of various diseases, including osteoporosis［8］. In recent years, multiple studies have shown that miRNAs can regulate bone formation and remodeling［9-11］.

Single-nucleotide polymorphism (SNP)-based genome-wide association studies (GWASs) have already identified approximately 100 BMD-associated loci［12］, including *CCDC170*. Multiple GWASs have shown that *CCDC170* is one of the genes most strongly linked to BMD across populations［13-15］. Recent study have found that multiple SNPs in *CCDC170* are associated with BMD, including rs6929137, rs371804, rs3734805, rs6932260, rs6904261, rs6932603, rs9383935,

rs9383589, rs3734806 and rs3757322［16］. The functions of most of these SNPs in vivo and in vitro remain unverified.

In the present study, we examined the role of *CCDC170* and miR-544a in osteosarcoma. We found that miR-544a differentially bound to the GWAS lead SNP rs6932603 (C-T) (in the *CCTC170* 3′-UTR) and inhibited osteogenesis by regulating the expressions of *RUNX2*, *OSX*, *ALP*, *COL1A1*, *Osteopontin* (*OPN*), *Osteocalcin* (*OCN*) and *Osteoprotegerin* (*OPG*). In summary, our study showed that rs6932603 may act as an etiological factor of osteoporosis and could be a possible target in treating osteoporosis.

Materials and methods

Cell cultures

The human embryonic kidney cell line, HEK293T, was obtained from the Cell Bank of Wuhan University (Wuhan, China). The human osteosarcoma cell line, U2OS, was purchased from the Cell Bank of the Chinese Academy of Sciences (Shanghai, China). HEK293T cells were cultured in Dulbecco's modified Eagle's medium (DMEM) (HyClone, Waltham, MA, USA), and U-2OS cells were grown in McCoy's 5A medium (HyClone). Media were supplemented with 10% fetal bovine serum (Invitrogen, Carlsbad, CA, USA), 100 U/ml penicillin, and 100 μg/ml streptomycin (Invitrogen). All cells were maintained at 37°C in a humidified incubator at 5% CO2.

Cell transfection and luciferase reporter assay

The rs6932603 C and T alleles were amplified and cloned into psi-check-2 vectors by inserting them between the SgfI/NotI sites. Table 1 shows the sequences cloned into the vectors. Cells were si-transfected with the rs6932603 C/T allele psi-check-2 vector or cotransfected with rs6932603C/T allele psi-check-2, miR-544a mimics, NC mimics, miR-544a inhibitors or NC inhibitors at 20 nM using Lipofectamine 3000 (Invitrogen) with serum-free media for 48h per the manufacturer's instructions. The luciferase reporter assay was performed using the Dual-Luciferase Reporter Assay (Yeasen); the relative luciferase activity was calculated after transfection for 48h by normalizing the Firefly luminescence to that of Renilla. Experiments were performed in triplicate, and all experiments were repeated three times. Table 1 lists the primer sequences.

RNA extraction and real-time polymerase chain reaction (PCR)

Cells were lysed, and total RNA was extracted using TRIzol reagent (Invitrogen) per the manufacturer's protocol and transcribed into cDNA using ReverAid (Thermo Scientific). Real-time PCR was performed using Hieff qPCR SYBR Green Master Mix (High Rox Plus) (Yeasen). Table 2 lists the PCR primer sequences.

Statistical analysis

Data are presented as mean ± SD. Statistical differences between two groups were determined by the twotailed Student's t test. Statistical differences among groups were analyzed by one-way ANOVA followed by Student–Neuman–Keuls' multiple comparisons test. All experiments were performed independently at least three times with similar results, and representative experiments are shown. $P < 0.05$

was considered statistically significant. NS > 0.05, *P < 0.05, **P < 0.01, ***P < 0.001.

Results

Differences in rs6932603-C and -T allele expressions

To determine whether the rs6932603-C and rs6932603-T allele expressions differed, 293T and U2OS cells were transfected with the rs6932603-C and rs6932603-T allele psi-check-2 vectors. The luciferase reporter assay showed that the rs6932603-T allele expression level was significantly lower than that of the rs6932603-C allele in the 293T cells and U2OS cells (Figs. 1A and 1B).

MiR-544a differentially regulated the allele variants of rs6932603

Next, we tested a biological model in which miR-544a differentially regulated the C/T allele variants of rs6932603 in *CCDC170*. In this model, rs6932603-T decreased the *CCDC170* transcription levels, leading to an increased osteoporosis risk as predicted (http://mirdsnp.ccr.buffalo.edu/ (Fig. 2A). To test our model, we cotransfected the rs6932603-C/T allele psi-check-2 vector, miR-544a mimics and NC mimics in 293T cells and U2OS cells. The luciferase reporter assay results showed that the miR-544a mimics significantly downregulated rs6932603-T expression in both cell lines (Figs. 2B and 2C). As an additional test of our model, the rs6932603-C/T allele psi-check-2 vector, miR-544a inhibitors and NC inhibitors were cotransfected into 293T cells and U2OS cells. The rs6932603-T expression was significantly upregulated in both cell lines (Figs. 2D and 2E). These results indicated that miR-544a inhibits *CCDC170* expression by differentially binding

rs6932603-C/T.

MiR-544a overexpression repressed the expression of osteogenesis marker genes

To explore the functional role of miR-544a in osteosarcoma and osteoporosis, miR-544a mimics and NC mimics were transfected into U2OS cells. qRT-PCR showed that expressions of the osteogenesis early-stage marker genes, *Runx2* and *Osterix*, the osteogenesis medium-stage marker genes, *Alp* and *Col1a1*, and the osteogenesis late-stage marker genes, *OPN* and *OCN*, were significantly downregulated (Figs. 3A–3F). We also found that osteoclastogenesis inhibitory factor (*OPG*) expression was significantly downregulated (Fig. 3G). These results indicated that miR-544a overexpression inhibited osteogenesis and promoted osteoclastogenesis.

MiR-544a knockdown increased the expression of osteogenesis marker genes

To further verify the role of miRNA in inhibiting osteogenesis and promoting osteoclastogenesis, miR-544a inhibitors and NC inhibitors were transfected into U2OS cells. By qRT-PCR, we found that the expressions of *Runx2*, *Osterix*, *Alp*, *Col1a1*, *OPN* and *OCN* were significantly upregulated (Figs. 4A–4F). We also found that *OPG* expression was significantly upregulated (Fig. 3G). These results indicated that knockdown-expression of miR-544a promoted osteogenesis and inhibited osteoclastogenesis.

Discussion

Identifying target genes is pivotal to understanding miRNA's roles in various

diseases, including osteoporosis［17］. The TargetScan, miRNASNP and miRbase databases were used to identify direct targets of miR-544a. *CCDC170* was predicted as one target of miR-544a. In our study, we found that miR-544a differentially regulated the allele variants of rs6932603-C/T in the *CCDC170* 3′-UTR via the luciferase reporter assay. Our study provided a possible mechanism for this, in that upregulation of miR-544a resulted in decreased *CCDC170* expression in osteoporosis. Multiple studies have found that *CCDC170* plays an important role in breast cancer ［18,19］and multiple genome-wide linkage scans have shown that *CCDC170* is one of the genes most strongly linked to BMD. However, no in vivo or in vitro experiments have directly verified the role of *CCDC170*. We plan to study this in our next research project.

MicroRNAs influence posttranscriptional regulation in various genes, and some have been shown to influence osteoporosis［20,21］. MiR-544a has been shown to play an important role in many diseases such as lung cancer and breast cancer, but its role in osteoporosis is unknown［22,23］. Here, we showed that miR-544a suppressed osteogenesis and promoted osteoclastogenesis by downregulating the expressions of *RUNX2*, *Osterix*, *ALP, Col1a1*, *OPN*, *OCN* and *OPG*.

In conclusion, our study demonstrated that miR-544a inhibits *CCDC170* expression by differentially binding rs6932603-C/T. MiR-544a also suppresses osteogenesis and promotes osteoclastogenesis by downregulating the expressions of osteogenesis marker genes. These findings may improve our understanding of the association between miRNAs, GWAD lead SNPs, and osteoporosis pathogenesis and

may provide a potential therapeutic target for osteoporosis therapy.

References

1. Sobacchi C, Schulz A, Coxon FP, Villa A, Helfrich MH. (2013) Osteopetrosis: genetics, treatment and new insights into osteoclast function. Nature Reviews Endocrinology 9:522–536. doi: 10.1038/nrendo.2013.137 PMID: 23877423
2. Albagha O. (2003) Genetic determinants of susceptibility to osteoporosis. Endocrinology and Metabolism Clinics of North America 32:65-81. doi: 10.1016/S0889-8529(02)00059-2 PMID: 12699293
3. Bing Mei, Ya Wang, Weiyuan Ye, Han Huang, Qian Zhou, et al. (2019) LncRNA ZBTB40-IT1 modulated by osteoporosis GWAS risk SNPs suppresses osteogenesis. Human Genetics 138:151-166. doi: 10.1007/s00439-019-01969-y PMID: 30661131
4. Ambros, Victor. (2004) The functions of animal microRNAs. Nature 431:350–355. doi: 10.1038/nature02871 PMID: 15372042
5. Ameres S L, Zamore P D. (2013) Diversifying microRNA sequence and function. Nature Reviews Molecular Cell Biology 14: 475–488. doi: 10.1038/nrm3611 PMID: 23800994
6. Mohr A M, Mott J L. (2015) Overview of microRNA biology. Seminars in Liver Disease 35:003-011. doi: 10.1055/s-0034-1397344 PMID: 25632930
7. Lou S, Sun T, Li H, Hu Z. (2018) Mechanisms of microRNA-mediated gene

regulation in unicellular model alga Chlamydomonas reinhardtii. Biotechnology for Biofuels 11:244. doi: 10.1186/s13068-018-1249-y PMID: 30202439

8. Paul P, Chakraborty A, Sarkar D, Langthasa M, Rahman M, et al. (2018) Interplay between miRNAs and human diseases. Journal of Cellular Physiology 233:2007-2018. doi: 10.1002/jcp.25854 PMID: 28181241
9. Zhao X, Xu D, Li Y, Liu T, Ji Y, et al. (2014) MicroRNAs regulate bone metabolism. Journal of Bone and Mineral Metabolism 32:221-231. doi: 10.1007/s00774-013-0537-7 PMID: 24311309
10. Kim K M, Lim S K. (2014) Role of miRNAs in bone and their potential as therapeutic targets. Current Opinion in Pharmacology 16:133-141. doi: 10.1016/j.coph.2014.05.001 PMID: 24907412
11. Cui Q, Xing J, Yu M, Wang Y, Xu J, et al. (2019) Mmu-miR-185 depletion promotes osteogenic differentiation and suppresses bone loss in osteoporosis through the Bgn-mediated BMP/Smad pathway. Cell Death Disease 10:172. doi: 10.1038/s41419-019-1428-1 PMID: 30787286
12. Mo XB, Lu X, Zhang YH, Zhang ZL, Deng FY, et al. (2015) Gene-based association analysis identified novel genes associated with bone mineral density. PLOS ONE 10:e0121811. doi: 10.1371/journal.pone.0121811 PMID: 25811989
13. Mullin BH, Walsh JP, Zheng HF, Brown SJ, Surdulescu GL, et al. (2016) Genome-wide association study using family-based cohorts identifies the WLS and CCDC170/ESR1 loci as associated with bone mineral density. BMC Genomics 17:136. doi: 10.1186/s12864-016-2481-0 PMID: 26911590

14. Villalobos CM, Jiménez RF, Karol E , Parra AY, González MA, et al. (2017) A pilot genome-wide association study in postmenopausal Mexican-Mestizo women implicates the RMND1/CCDC170 locus is associated with bone mineral density. International Journal of Genomics 2017:1-13. doi: 10.1155/2017/5831020 PMID: 28840121

15. Hidalgo BA, Parra AY, Casas AL, Jimenez RF, Ramírez EG, et al. (2019) Association of RMND1/CCDC170-ESR1 single nucleotide polymorphisms with hip fracture and osteoporosis in postmenopausal women. Climacteric: the journal of the International Menopause Society 22:97-104. doi: 10.1080/13697137.2018.1538339 PMID: 30601066

16. Qin L, Liu Y, Wang Y, Wu G, Chen J, et al. (2016) Computational Characterization of Osteoporosis Associated SNPs and Genes Identified by Genome-Wide Association Studies. PLOS ONE 11:e0150070. doi: 10.1371/journal.pone.0150070 PMID: 26930606

17. Saetrom P, Biesinger J, Li SM, Smith D, Thomas LF, et al. (2009) A Risk Variant in an miR-125b Binding Site in BMPR1B Is Associated with Breast Cancer Pathogenesis. Cancer Research 69:7459-7465. doi: 10.1158/0008-5472.CAN-09-1201 PMID: 19738052

18. Jiang P, Li Y, Poleshko A, Medvedeva V, Baulina N, et al. (2007) The Protein Encoded by the CCDC170 Breast Cancer Gene Functions to Organize the Golgi-Microtubule Network. EBioMedicine 22:28-43. doi: 10.1016/j.ebiom.2017.06.024 PMID: 28687497

19. Fimereli D, Fumagalli D, Brown D, Gacquer D, Rothé F, et al. (2018) Genomic hotspots but few recurrent fusion genes in breast cancer. Genes, Chromosomes and Cancer 57:331-338. doi: 10.1002/gcc.22533 PMID: 29436103

20. Jones KB, Salah Z, Del Mare S, Galasso M, Gaudio E, et al. (2012) MiRNA signatures associate with pathogenesis and progression of osteosarcoma. Cancer Research 72:1865-1877. doi: 10.1158/0008-5472.CAN-11-2663 PMID: 22350417

21. Lian F, Cui Y, Zhou C, Gao K, Wu L. (2015) Identification of a Plasma Four-microRNA Panel as Potential Noninvasive Biomarker for Osteosarcoma. PLOS ONE 16;10:e0121499. doi: 10.1371/journal.pone.0121499 PMID: 25775010

22. Lu P, Gu Y, Li L, Wang F, Qiu X. (2016) MiR-544a Promotes Breast Cancer Cell Migration and Invasion Reducing Cadherin 1 Expression. Oncology Research 23:165. doi: 10.3727/096504016X14519157902726 PMID: 27053345

23. Wang A, Zhao C, Gao Y, Duan G, Yang Y, et al. (2019) LEF1-AS1 contributes to proliferation and invasion through regulating miR-544a/ FOXP1 axis in lung cancer. Investigational New Drug 8. doi: 10.1007/s10637-018-00721-z PMID: 30734202

Table 1. Small fragments of RNA synthesized in the present study

Name	*Sequences (5'–3')*
miR-544a mimics	AUUCUGCAUUUUUAGCAAGUUC
NC mimics	UUCUUCGAACGUGUCACGUTT
miR-544a inhibitors	GAACUUGCUAAAAAUGCAGAAU
NC inhibitors	CAGUACUUUUGUGUAGUACAA
rs6932603C-F	CGCAAAAGCCATACCTCTTCTCCTGCTACGCA
	GAATCTGTTTCTCCTGAATCTC GC
rs6932603C-R	GGCCGCGAGATTCAGGAGAAACAGATTCTGC
	GTAGCAGGAGAAGAGGTATGGCTTTTGCGAT
rs6932603T-F	CGCAAAAGCCATACCTCTTCTCCTGCTATGCA
	GAATCTGTTTCTCCTGAATCTC GC
rs6932603T-R	GGCCGCGAGATTCAGGAGAAACAGATTCTGC
	ATAGCAGGAGAAGAGGTATGGCTTTTGCGAT

Table 2. PCR primers sequences in the present study

Name	*Sequences (5'–3')*	*Temperature*
GADPH-F	TCAAGAAGGTGGTGAAGCAGG	---
GADPH-R	AGCGTCAAAGGTGGAGGAGTG	---
Runx2-F	TCTTCACAAATCCTCCCC	52℃
Runx2-R	TGGATTAAAAGGACTTGG	52℃
Osterix-F	CACAGCTCTTCTGACTGTCT	52℃
Osterix-R	GGTGAAATGCCTGCATGGAT	52℃
Alp-F	GACAAGAAGCCCTTCACTGC	59℃
Alp-R	AGACTGCGCCTGGTAGTTGT	59℃
Col1a1-F	CATCTCCCCTTCGTTTTTGA	59℃
Col1a1-R	CCAAATCCGATGTTTCTGCT	59℃
OPN-F	ACTCGAACGACTCTGATGATGT	57℃
OPN-R	GTCAGGTCTGCGAAACTTCTTA	57℃
OCN-F	GCAAGTAGCGCCAATCTAGG	59℃
OCN-R	GCTTCACCCTCGAAATGGTA	59℃
OPG-F	CACAAATTGCAGTGTCTTTGGTC	53℃
OPG-R	TCTGCGTTTACTTTGGTGCCA	53℃

Figure legends

Fig. 1. Expression differences between the rs6932603-C and -T alleles. (A) Expression level of the rs6932603-T allele was significantly lower than that of the C allele in 293T cells. (B) Expression level of the rs6932603-T allele was significantly lower than that of the C allele in U2OS cells. Results are shown as percentages relative to luciferase activity. Data are from three independent transfection experiments with assays performed in triplicate (n=6). Luciferase signaling was normalized to Renilla signaling. Error bars show the standard deviation for six technical replicates of a representative experiment. P-values were calculated using a two-tailed Student's t-test. ***P<0.001.

Fig. 2. MiR-544a differentially regulates the allele variants of rs6932603. (A) Schematic diagram of the miR-544a binding site on *CCDC170*. (B) Overexpression of miR-544a significantly suppressed rs6932603-T allele levels in 293T cells. (C) Overexpression of miR-544a significantly suppressed rs6932603-T allele levels in U2OS cells. (D) Knockdown of miR-544a significantly upregulated rs6932603-T allele levels in 293T cells. (E) Knockdown of miR-544a significantly upregulated rs6932603-T allele levels in U2OS cells. Results are shown as percentages relative to luciferase activity. Data are from three independent transfection experiments with assays performed in triplicate (n=6). Luciferase signaling was normalized to Renilla

signaling. Error bars show the standard deviation for six technical replicates of a representative experiment. P-values were calculated using a two-tailed Student's t-test. ***P<0.001.

Fig. 3. MiR-544a overexpression repressed the expression of osteogenesis marker genes. (A-B) Overexpression of miR-544a significantly suppressed the expression of *Runx2* and *Osterix*. (C-D) Overexpression of miR-544a significantly suppressed the expression of *Alp* and *Col1a1*. (E-F) Overexpression of miR-544a significantly suppressed the expression of *OPN* and *OCN*. (G) Overexpression of miR-544a significantly suppressed the expressions of *OPN* and *OPG*. Data are from three independent transfection experiments with assays performed in triplicate (n=8). Error bars show the standard deviation for four technical replicates of a representative experiment. P values were calculated using a two-tailed Student's t-test. **P<0.01,***P<0.001.

Fig. 4. MiR-544a knockdown increased the expressions of osteogenesis marker genes. (A-B) Knockdown-expression of miR-544a significantly increased the expressions of *Runx2* and *Osterix*. (C-D) Knockdown-expression of miR-544a significantly increased *Alp* and *Col1a1* expression. (E-F) Knockdown-expression of miR-544a significantly increased the expressions of OPN and OCN. (G) Knockdown-expression of miR-544a significantly increased *OPG* expression. Data are from three independent transfection experiments with assays performed in triplicate (n=8). Error bars show the standard deviation for four technical replicates of a representative experiment. P-values were calculated using a two-tailed Student's

t-test. ** P<0.01,***P<0.001.

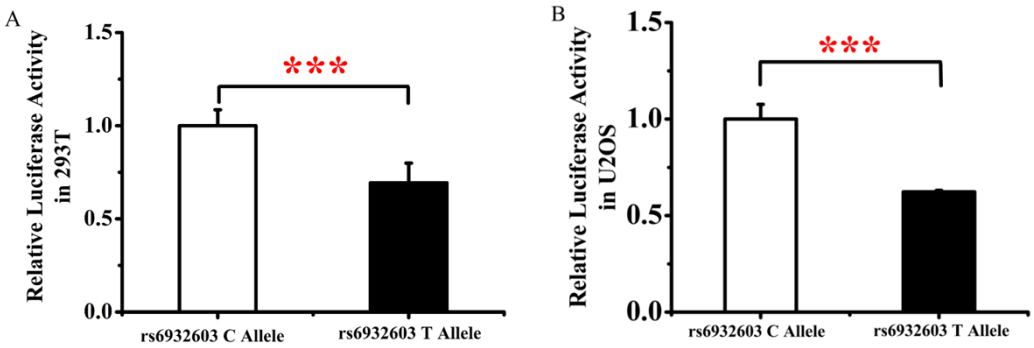

Fig. 1

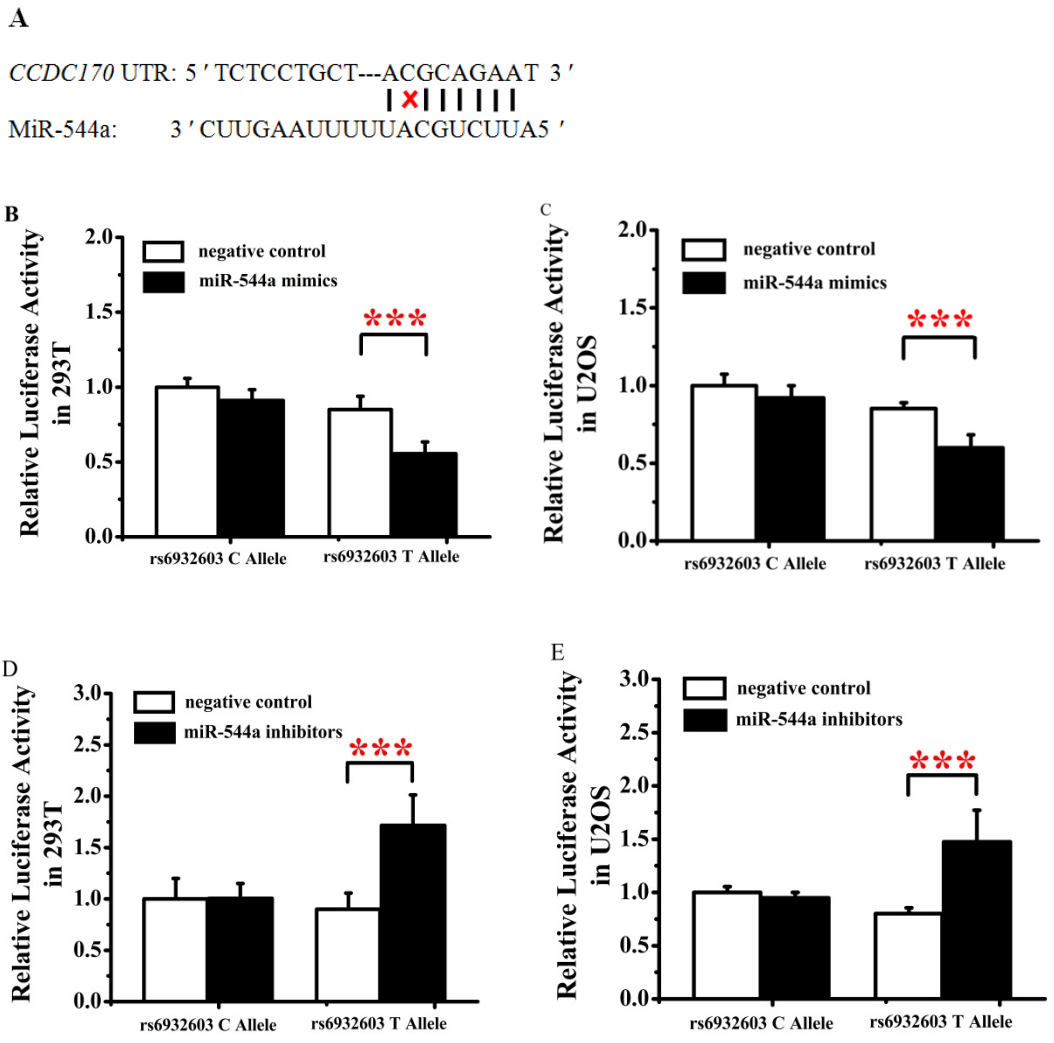

Fig. 2

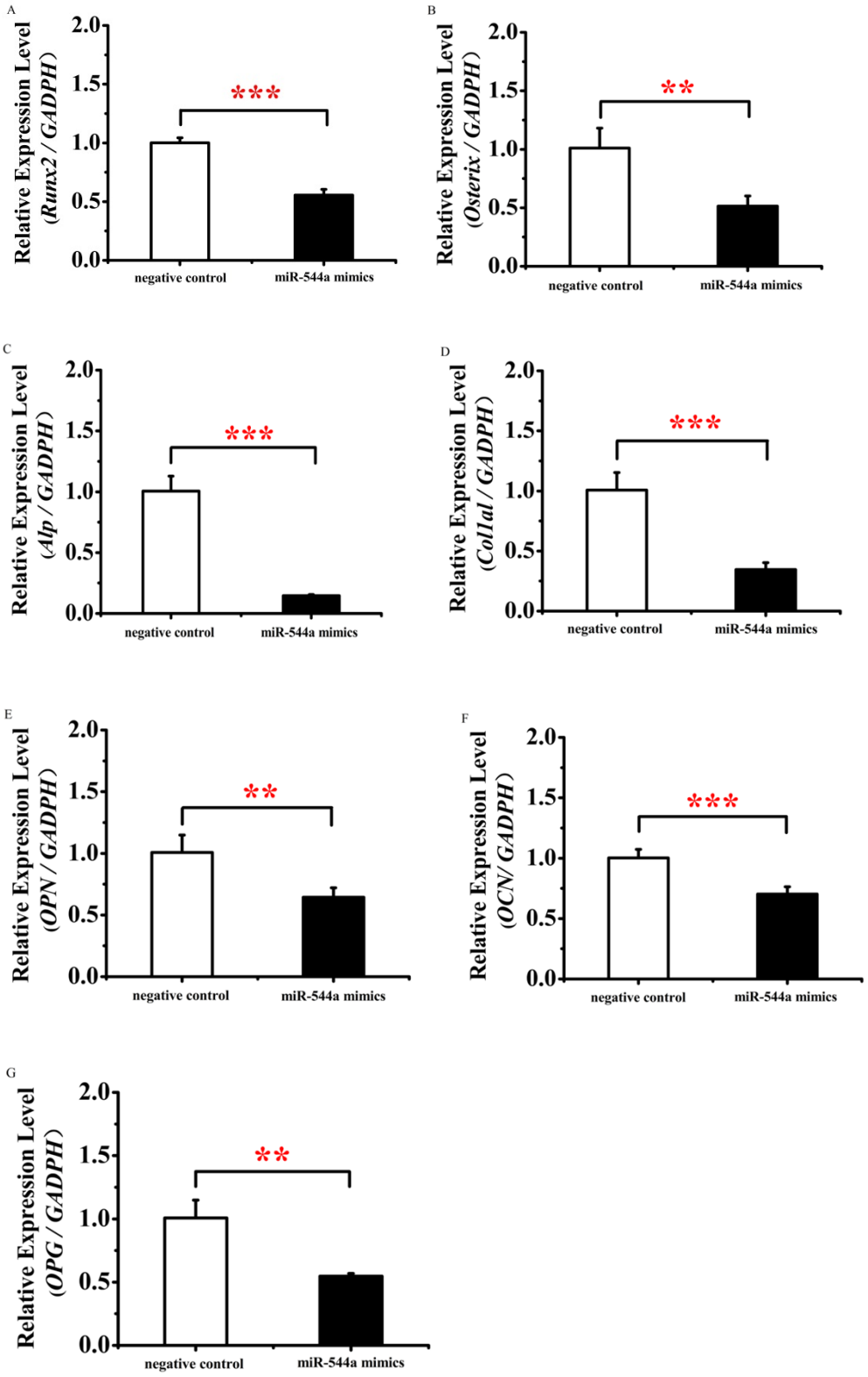

Fig. 3

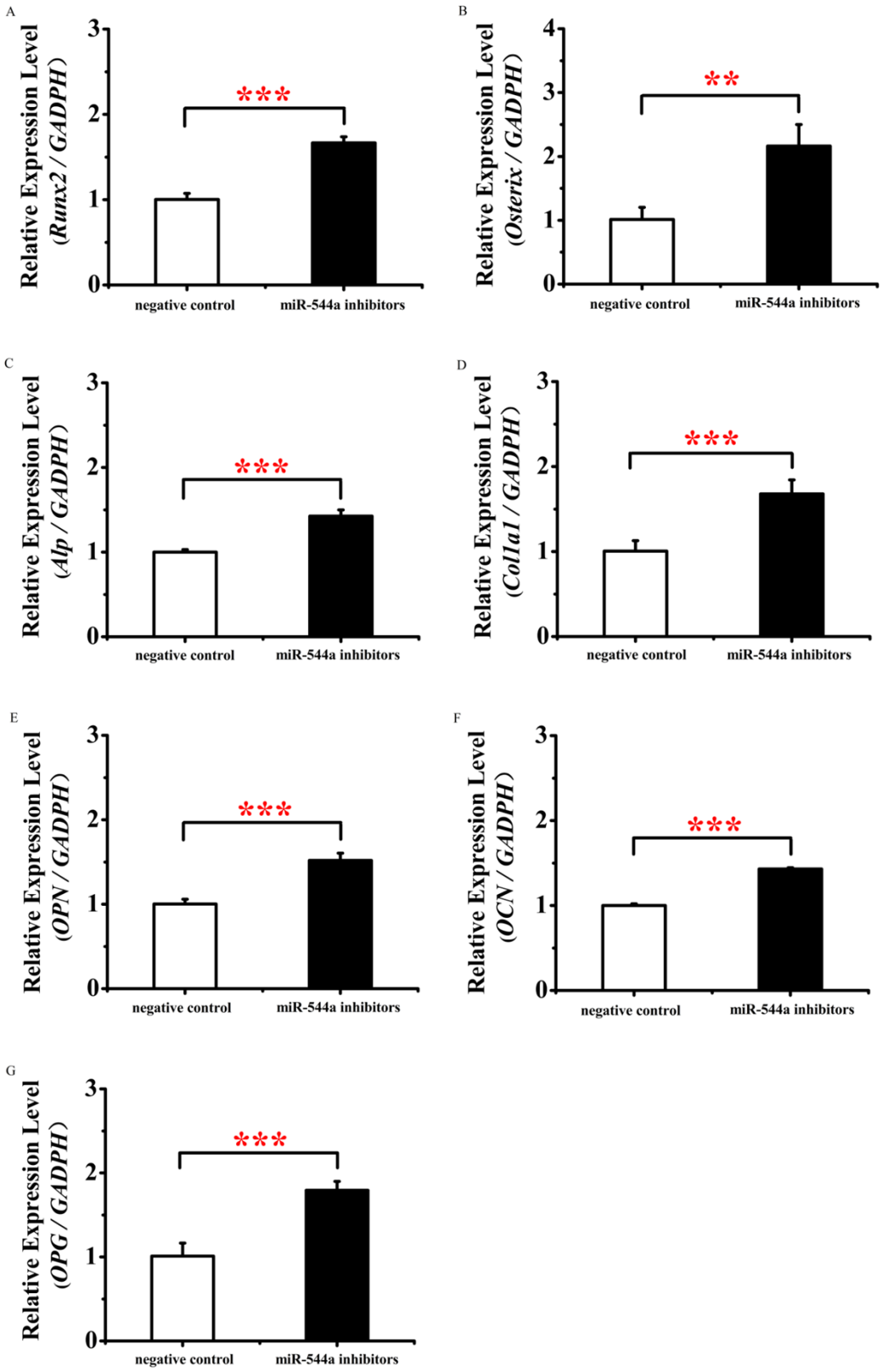

Fig. 4

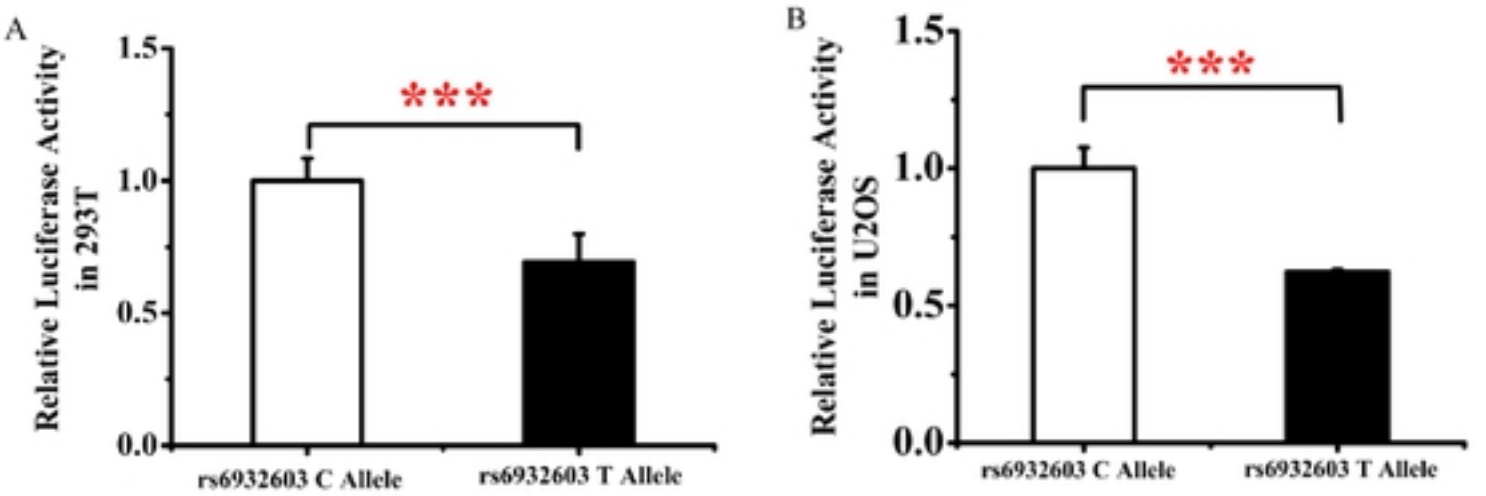

Fig. 1

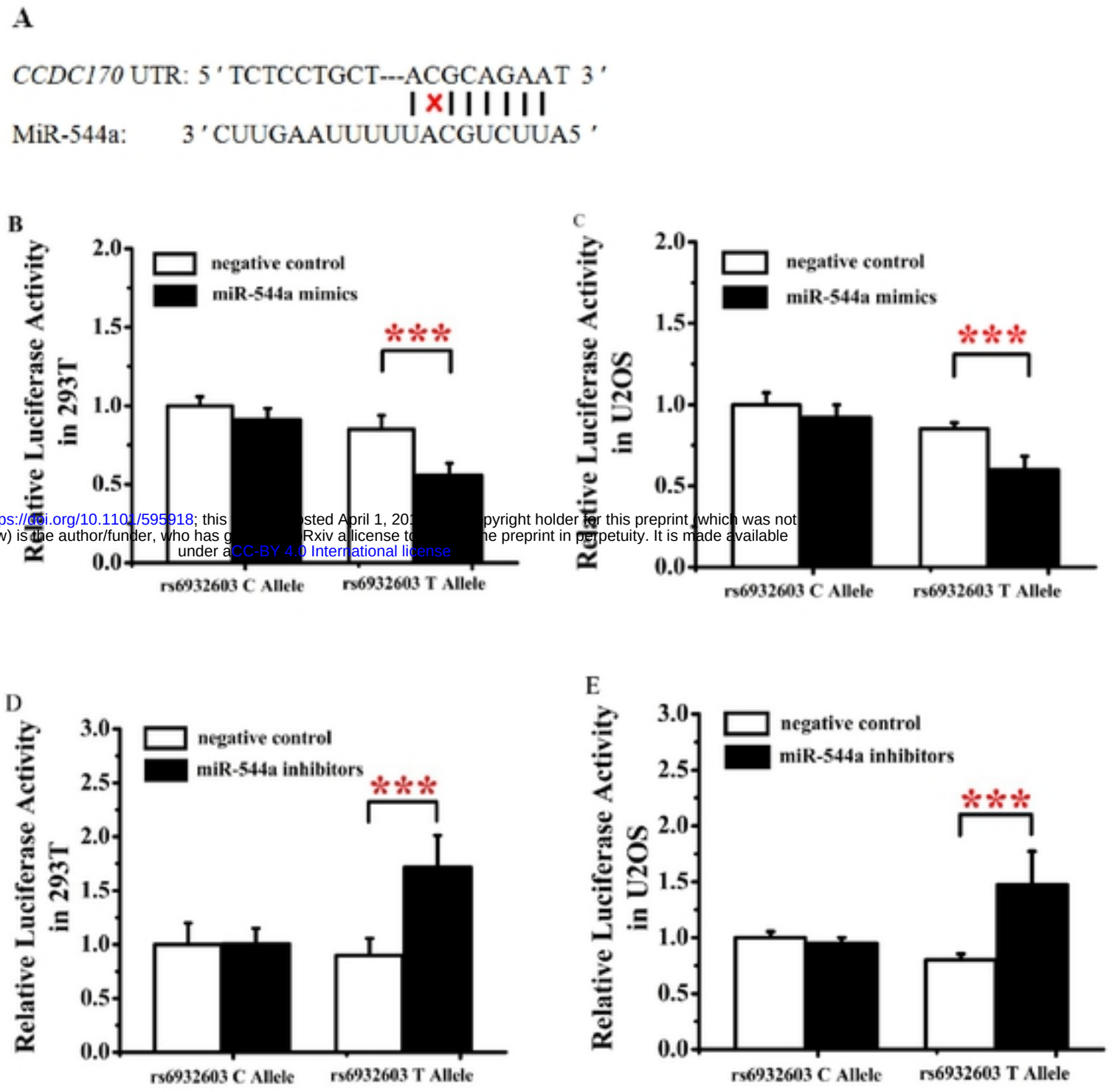

Fig. 2

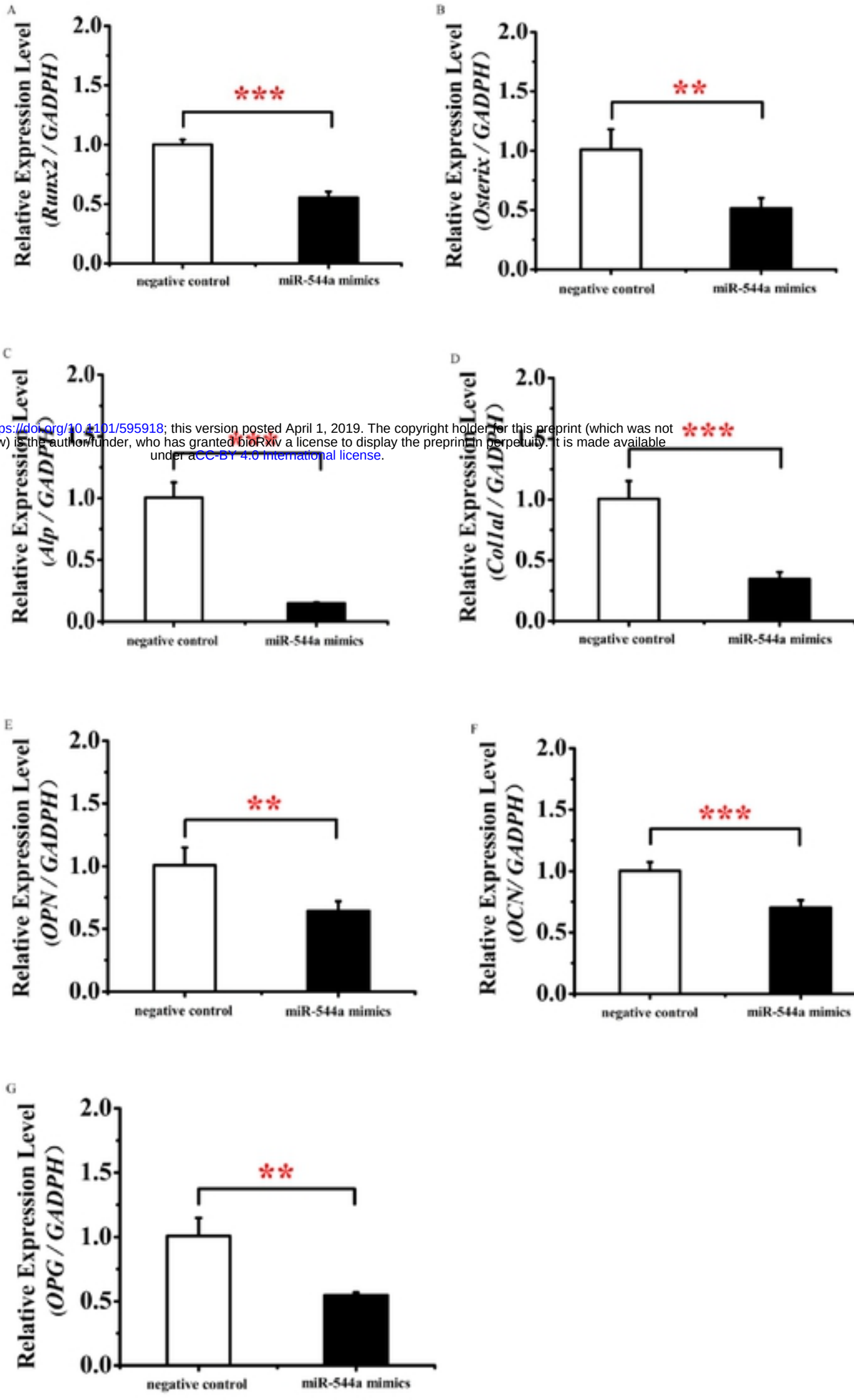

Fig. 3

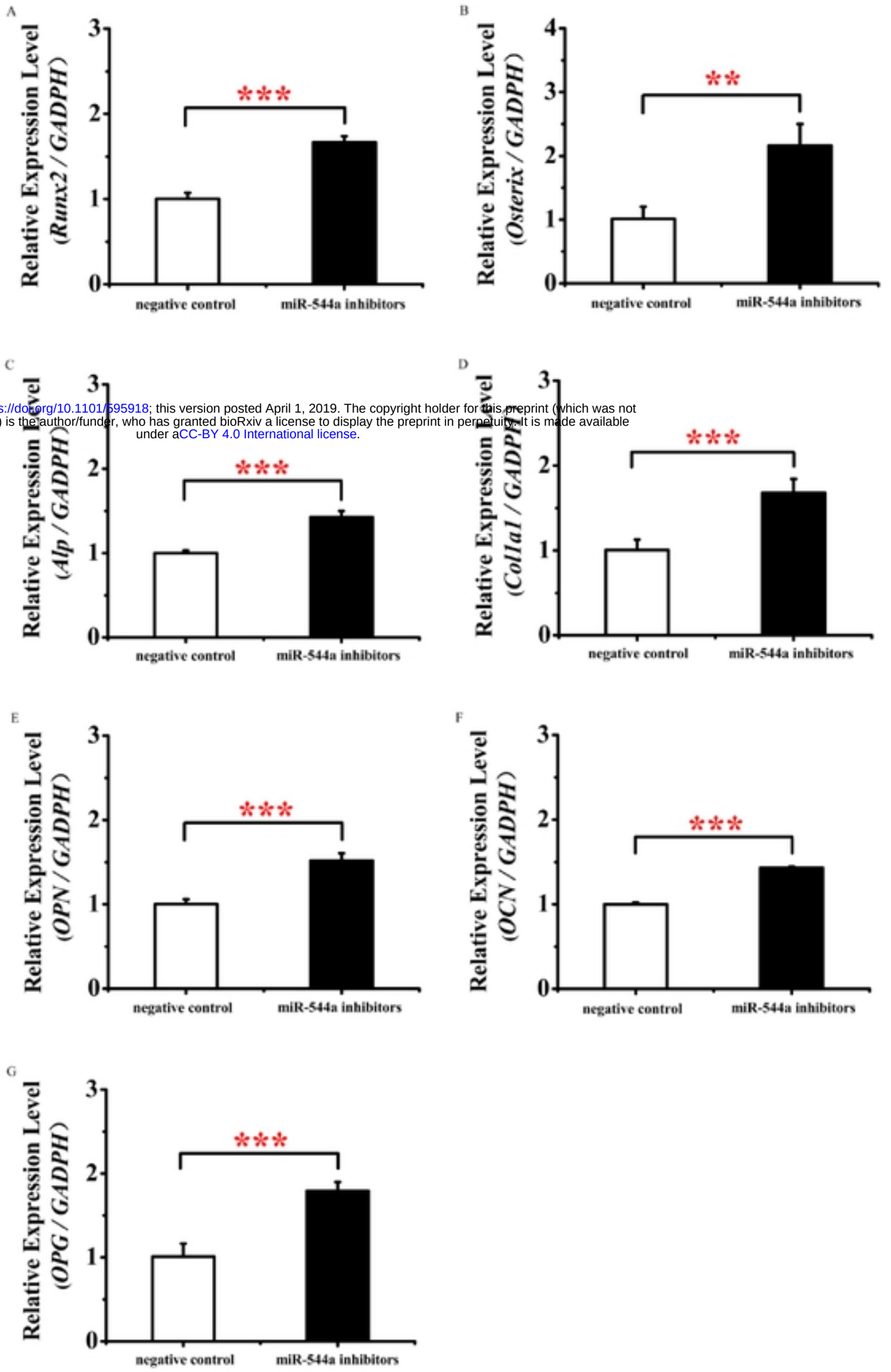

Fig. 4